Photogrammetrie • Fernerkundung • Geoinformation 6/2006, S. 469–480, 7 figs., 1 tab.

Three-Dimensional Reconstruction of Bathymetry using C-band TOPSAR Data

MAGED MARGHANY & MAZLAN HASHIM, Skudai, Johore Bahru, Malaysia

Keywords: Photogrammetry, remote sensing, bathymetry, SAR, TOPSAR, Malaysia

Abstract: This paper reports on a study carried out for the generation of three-dimensional (3D) ocean bathymetry using airborne TOPSAR data. The main objective of this study is to utilize Fuzzy arithmetic for constructing ocean bathymetry from polarized remote sensing data such as a TOPSAR image. In doing so, two three-dimensional surface models, the Volterra model and a Fuzzy B-Spline model which construct a global topological structure between the data points were used to support an approximation of real surface. The best reconstruction of coastal bathymetry of the test site in Kuala Terengganu, Malaysia, was obtained with polarized C bands TOPSAR acquired with VV polarization. With 10 m spatial resolution of TOPSAR data, an accuracy of (root mean square) ± 9 m was found with C_{vv} band.

Zusammenfassung: *Die dreidimensionale Rekonstruktion der Unterwasser-Geländeformen mit Hilfe von TOPSAR-Daten im C-Band.* In diesem Beitrag werden die Ergebnisse einer Studie vorgestellt. Insbesondere wird die Verwendung der Fuzzy-Arithmetik für die Darstellung des Tiefenreliefs aus polarisierten Fernerkundungsdaten, wie z. B. TOPSAR-Bildern, erläutert. Für diesen Zweck wurden zwei dreidimensionale Oberflächenmodelle verwendet – das Volterra-Modell und ein Fuzzy B-Spline-Modell – mit deren Hilfe eine globale topographische Struktur erzeugt wurde zur Herstellung von Approximationen für die wirkliche Geländeoberfläche. Das beste Ergebnis der Rekonstruktion des Testgebietes bei Kuala Terengganu wurde mit den TOPSAR C Band-Daten mit VV Polarisierung erreicht. Mit 10 m räumlicher Auflösung der TOPSAR-Daten wurde im C_{VV}-Band eine Genauigkeit (rms) von ± 9 m erreicht.

1 Introduction

The operational use of Synthetic Aperture Radar (SAR) on coastal bathymetry mapping is of interest for a diversity of end users (HENNINGS et al. 1989). It is considered to provide key parameters for coastal engineering and coastal navigation. It is also valuable towards economic activities, security and marine environmental protection (VOGELZANG et al. 1992, VOGELZANG et al. 1997, HESSELMANS et al. 2000).

Remote sensing methods in real time could be a major tool for bathymetry mapping which could produce a synoptic impression over large areas at comparatively low cost. The ocean bathymetry features can be imaged by radar in coastal waters with strong tidal currents. Several theories concerning radar imaging mechanism of underwater bathymetry have been established by ALPERS & HENNINGS (1984), SHUCHMAN et al. (1985), and VOGELZANG et al. (1997). The imaging mechanism, which simulate under water topography from a given SAR image consists of three models: flow, wave and SAR backscatter models. These theories are on the basis of commercial services, which generate bathymetric charts by inverting SAR images at a significantly lower cost than conventional survey techniques (WENSINK & CAMPBELL 1997). In this context,

1432-8364/06/2006/0469 $ 3.00

Hesselmans et al. (2000) developed Bathymetry Assessment System, a computer program, used to calculate the depth from any SAR images, with limited number of sounding data. From their findings, imaging model was suitable for simulating a SAR image from the depth map. It showed good agreement between the backscatters in both the simulated and airborne-acquired images, when compared, with accuracy (root mean square) error of ± 0.23 m within a coastal bathymetry range of 25–30 m. Inglada & Garello (1999 and 2002) introduced a nonlinear tool, Volterra model to reconstruct 3-D bathymetry based on surface current velocity. In contrast to this, there are three main limitations of this technique, namely: (i)require high computational effort/task during the inverse model, (ii) the effects of linear components cannot be verified due to nonlinearity of SAR image; and (iii) the requirement to discretization of Volterra model using appropriate numerical analysis such as Euler and Lagrangian finite element for simulating the sea surface current. Further to that, the grid procedures are needed to reconstruct 3-D bottom topography from 2-D Volterra model inputs into a continuity equation. In this context, this paper addresses an approach for overcoming the abovementioned shortcomings. The contributions of this work can be summarized as follows: (i) minimise uncertainties of Volterra output due to nonlinearity that inherent in real ocean variation and SAR data, (ii) to introduce robust approach for reconstructing 3-D bathymetry based on Fuzzy B-spline model, compared to of which both approaches use not given in the Inglada & Garello (1999 and 2002), and (iii) to demonstrate the utilize of Fuzzy B-spline model to reconstruct 3-D of bathymetry from complex data without the use of the well known grid procedures.

In addition, we also emphasize how 3-D coastal water bathymetry can be reconstructed using a single airborne SAR data (namely the TOPSAR) with the integration of Volterra kernel (Inglada & Garello 1999) and Fuzzy B-spline models (Maged et al. 2002). Three hypotheses are examined: (i) the use of Volterra model to detect ocean surface current from C band TOPSAR with VV polarization, (ii) the use of continuity equation model to obtain the water depth, and (iii) the use of Fuzzy B-spline model to invert water depth values obtained by the continuity equation into 3-D bathymetry.

2 Methodology

2.1 *Data Set*

The Jet Propulsion Laboratory (JPL) airborne Topographic Synthetic Aperture Radar (TOPSAR) data were acquired on December 6, 1996 over the coastline of Kuala Terengganu, Malaysia between 103° 5′ E to 103° 9′ E and 5° 20′ N to 5° 27′ N. TOPSAR is a NASA/JPL multi-frequency radar imaging system aboard a DC-8 aircraft. It is operated by NASA's Armes research Center at Moffett Field, USA. TOPSAR data are fully polarimetric SAR data acquired with HH-, VV-, HV- and VH-polarized signals from 5 m × 5 m pixels, recorded for three wavelengths: C band (5 cm), L band (24 cm) and P band (68 cm) at 10 m spatial resolution. A further explanation of TOPSAR data acquisition can be found in Melba et al. (1999). This study utilizes C_{vv} band for 3-D bathymetry reconstruction because of the widely known facts of the good interaction of VV polarization to oceanographic physical elements such as ocean wave, surface current features, etc. Elaboration of such further explanation can be found in (Hesselmans et al. 2000 and Inglada & Garello 2002).

2.2 *3-D Coastal Water Bathymetry Model*

There are two models involved for bathymetric simulation: Volterra and Fuzzy B-spline models. The current velocity is simulated by using Volterra model in which it could be used with the continuity equation in order to derive water depth variations. On the other hand the Fuzzy B-spline is used to reconstruct 2-D water depth to 3-D dimensional (Fig. 1).

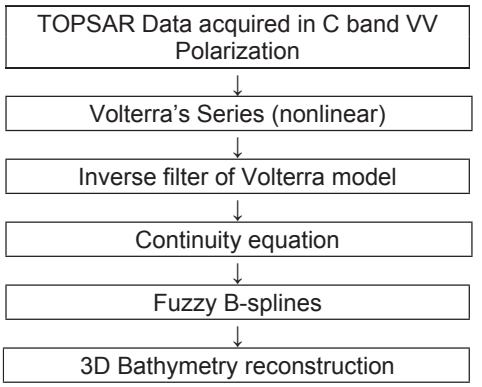

Fig. 1: Flow Chart of 3-D Bathymetry Reconstruction.

2.3 *Volterra Model*

The primary purpose of Volterra model is to express SAR image intensity as a series of nonlinear filters on the actual ocean surface. This model can be used to study the image energy variation as a function of parameters such as current direction or current waveform. A generalized, nonparametric framework to describe the input–output x and y signal relation of a time-invariant nonlinear system is provided by Inglada & Garello (1999). In discrete form, the Volterra series for input, $x(n)$, and output, $y(n)$ as given by Inglada & Garello (1999) can be expressed as:

$$\begin{aligned} Y(n) = h_0 + \sum_{i_1=1}^{\infty} h_1(i_1)\, X(n-i_1) + \\ + \sum_{i_1=1}^{\infty}\sum_{i_2=1}^{\infty} h_2(i_1,i_2)\, X(n-i_1)\, X(n-i_2) + \\ + \sum_{i_1=1}^{\infty}\sum_{i_2=1}^{\infty}\sum_{i_3=1}^{\infty} h_3(i_1,i_2,i_3)\, X(n-i_1) \\ X(n-i_2)\, X(n-i_3) + \\ + \ldots + \\ + \sum_{i_1=1}^{\infty}\sum_{i_2=1}^{\infty}\cdots\sum_{i_k=1}^{\infty} h_k(i_1,i_2,\ldots i_k) \\ X(n-i_1)\, X(n-i_2)\ldots X(n-i_k) \end{aligned} \quad (1)$$

where zeroth-order Volterra kernel h_0 is a constant representing zero-input response of the system and n is a discrete time: i. e., discrete time increments are indexed from 0 (time 0) to n (time t), and the evaluation of Y at time n is denoted by $Y(n)$. In addition to that, $i_1, i_2, \ldots, i_k$, are the lags in input $X(n)$. This implies that Volterra series is a representation of output $Y(n)$ in terms of present and past values of input $X(n)$.The function $h_k(i_1, i_2, \ldots, i_k)$ is kth-order Volterra kernel characterizing the system. The h_1 is the kernel of the first order Volterra functional, which performs a linear operation on the input. This term is comparable on the basic of frequency response function of a linear system, transformed into the time domain. However, kernel h_1 gives a more accurate portrayal of a system's linear response, in comparison to frequency response function. This is because h_1 exists with the knowledge of higher-order, nonlinear terms while the frequency response function assumes a completely linear response. The h_2, h_3, …, h_k capture nonlinear interactions between input and output TOPSAR signals. Here the kernel is a function of time (n) and two distinct time lags. It is through these time lags that nonlinear kernels represent the effect of a previous response as it is carried through time in the system. The order of non-linearity is the highest effective order of multiple summations in the functional series. Following Schetzen (1980) Fourier transform is used to acquire nonlinearity function from equation 1 as given by

$$Y(v) = FT[Y(n)] = \int Y(n)\, e^{-j2\pi vn}\, dn \quad (2)$$

where v is frequency and $j = \sqrt{-1}$ (Inglada & Garello 2002). Domain frequency of TOPSAR image $I_{TOPSAR}(v, \Psi)$ can be described by using equation 2 with following expression

$$I_{TOPSAR}(v, \Psi_0) = FT[I(x,y)\, e^{j(R/V)\, u_Y(x,y)}] \quad (3)$$

where $I(x, y)$ is the intensity TOPSAR image pixel of azimuth (x) and range (y), respectively, ψ_0 is the wave spectra energy and R/V is the range to platform velocity ratio, in case of TOPSAR 32 s and $u_Y(x, y)$ is the radial component of surface velocities (In-

GLADA & GARELLO 2002). Nevertheless, equation 3 does not satisfy the relationship between TOPSAR image and ocean surface roughness. More precisely, the action balance equation (ABC) describes the relationship between surface velocity $\vec{U}(\vec{x})$, and its gradient and the action spectral density ψ of the short surface wave i. e. Bragg wave (ALPERS & HENNINGS 1984). In reference to INGLADA & GARELLO (1999), the expression of ABC into first-order Volterra kernel $H_{1y}(v_x, v_y)$ of frequency domain for the current flow in the range direction can be described as:

$$H_{1y}(v_x, v_y) = k_y \vec{U} \cdot \frac{\partial x}{\partial u_x} \cdot \cdot \left[\vec{K}^{-1} \left(\frac{\partial}{\partial t} + \frac{\partial \vec{c}_g}{\partial x} + \frac{\partial \vec{u}_x}{\partial x} \right) + 0.043 \frac{(\vec{u}_a \vec{K})^2}{\omega_0} \right] \cdot \cdot \left[\frac{\partial \psi}{\partial \omega} \right] \cdot \frac{\vec{c}_g(\vec{K})\, \vec{U} + j \cdot 0.043 (\vec{u}_a \vec{K})^2 \omega_0^{-1}}{[\vec{c}_g(\vec{K})\, \vec{U}]^2 + [0.043 (\vec{u}_a \vec{K})^2 \omega_0^{-1}]^2} + + j \cdot (0.6 \cdot 10^{-2} \cdot \vec{K}^{-4}) \left(\frac{R}{V} \right) \vec{u}_x \quad (4)$$

where $\vec{U}$ is the mean current velocity, $\vec{u}_x$ is the current flow while $\vec{u}_a$ is current gradient along azimuth direction, respectively. k_y is the wave number along range direction, $\vec{K}$ is the spectra wave number, ω_0 is the angular wave frequency, $\vec{c}_g$ is the wave velocity group, ψ is the wave spectra energy and R/V is the range to platform velocity ratio, in case of TOPSAR 32 s. Then, domain frequency of TOPSAR image $I_{TOPSAR}(v, \Psi)$ can be expressed by using Volterra model for ABE into equation 3 by following formula introduced by INGLADA & GARELLO (2002)

$$I_{TOPSAR\,V}(v, \Psi) = FT \left[\Psi_0(x, y) + \int Y(n) \cdot \sum_{N=0}^{+\infty} \frac{1}{n!} \left(j \frac{R}{V} u_Y(x, y) \right)^N \right] \quad (5)$$

where $N = 1, 2, 3, \ldots k$ and $I_{TOPSAR\,V}(v, \Psi)$ represents Volterra kernels for the TOPSAR image in frequency domain in which can be used to estimate current flow $U_y(0, y)$ in the range direction (y) with the following expression (INGLADA & GARELLO 2002)

$$I_{TOPSAR\,V} = U_y(0, y) \cdot H_{1y}(v_x, v_y) \quad (6)$$

In reference to INGLADA & GARELLO (1999), the inverse filter $G(v_x, v_y)$ is used since $H_{1y}(v_x, v_y)$ has a zero for (v_x, v_y) which indicates the mean current velocity should have a constant offset. The inverse filter $G(v_x, v_y)$ can be given as

$$G(v_x, v_y) = \begin{cases} [H_{1y}(v_x, v_y)]^{-1} & \text{If } (v_x, v_y) \neq 0, \\ 0 & \textit{otherwise}. \end{cases}$$

Using equation 6 into 7, range current velocity $U_y(0, y)$ can be estimated by

$$U_y(0, y) = I_{TOPSAR\,V} \cdot G(v_x, v_y) \quad (8)$$

Then, the continuity equation is used to estimate the water depth as given by VOGELZANG (1992)

$$\frac{\partial \zeta}{\partial t} + \nabla \cdot \{(d + \zeta)\, U_y(x, y)\} = 0 \quad (9)$$

where ζ is the surface elevation above the mean sea level, whereby it is obtained from tidal table, t is time and d is local water depth. The real current data was estimated from Malaysian tidal table of December 6, 1996.

2.4 *The Fuzzy B-splines Method*

Fuzzy numbers have been introduced with the use of Fuzzy-B-splines model, instead of intervals in the definition of B-splines. Typically, in computer graphics, there are two objective quality definitions for Fuzzy B-splines that are used: triangle-based and edge-based criteria. A Fuzzy number is defined using interval analysis. Given a data set S of sparse water depth data over a rectangular region D, we have partitioned D into a grid of m times n rectangular cells (ANILE et al. 1997). For each cell, a fuzzy number summarizing data has been computed. There are two basic notions that are combined together: confidence interval and presumption level. A confidence interval is a real values interval which provides the sharpest enclosing range for water depth (d) function of ocean current gradient values.

It is of an assumption μ-level is an estimated truth value in the [0,1] interval on our knowledge level of water depth variation over a region D (Anile 1997). The 0 value corresponds to minimum knowledge of water depth, and 1 to the maximum water depth. A Fuzzy number is then prearranged in confidence interval set, each one related to a presumption level $\mu \in [0, 1]$. Moreover, the following must hold each pair of confidence interval which defines a number: $\mu \succ \mu' \Rightarrow d \succ d'$. Let us consider a function $f: d \rightarrow d$, of N fuzzy variables $d_1, d_2, \ldots, d_N$. Where d_N are the global minimum and maximum water depth values which are function of the current gradient variation into the space (S). Based on the spatial variation of gradient current, and water depth, the algorithms are used to compute the function f.

Let $d(i,j)$ be the depth value at location i,j in the region D where i is the horizontal and j is the vertical coordinates of a grid of m times n rectangular cells. Let N be the set of eight neighboring cells (Fig. 2). The input variables of the fuzzy are the amplitude differences of water depth d defined by (Anile et al. 1997):

$$\Delta d_i = d_i - d_0, \quad i = 1, \ldots, 8 \tag{10}$$

where the d_i, $N = 1, \ldots, 8$ values are the neighboring cells of the actually processed cell d_0 along the horizontal coordinate i. To estimate the fuzzy number of water depth d_j which is located along the vertical coordinate j, we estimated the membership function values μ and μ' of the fuzzy variables d_i and d_j, respectively by the following equations were described by Rövid et al. (2004)

$$\mu = \max\{\min\{m_{pl}(\Delta d_i) : d_i \in N_i\}; N = 1, \ldots, 9\} \tag{11}$$

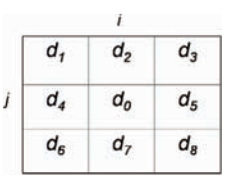

Fig. 2: Grid used to obtain Fuzzy number in i and j coordinates.

$$\mu' = \max\{\min\{m_{LNl}(\Delta d_i) : d_i \in N_i\}; N = 1, \ldots, 9\} \tag{12}$$

where m_{pl} and m_{LNl} correspond to the membership functions of fuzzy sets. From equations 11 and 12, one can estimate the fuzzy number of water depth d_j

$$d_j = d_i + (L - 1)\,\Delta\mu \tag{13}$$

where $\Delta\mu$ is $\mu - \mu'$ and $L = \{d_1, \ldots, d_N\}$. Equations 12 and 13 represent water depth in 2-D, in order to reconstruct fuzzy values of water depth in 3-D, then fuzzy number of water depth in z coordinate is estimated by the following equation proposed by Russo (1998),

$$d_z = \Delta\mu\, MAX\{m_{LA}|d_{i-1,j} - d_{i,j}|, m_{LA}|d_{i,j-1} - d_{i,j}|\} \tag{14}$$

where d_z fuzzy water depth value in z coordinate which is function of i and j coordinates i. e. $d_z = F(d_i, d_j)$. Fuzzy number F_O for water depth in i,j and z coordinates then can be given by

$$F_O = \{\min(d_{z_0}, \ldots, d_{z_\Omega}), \max(d_{z_0}, \ldots, d_{z_\Omega})\} \tag{15}$$

where $\Omega = 1, 2, 3, 4, \ldots,$

The fuzzy number of water depth F_O then defined by B-spline in order to reconstruct 3-D of water depth. In doing so, B-spline functions including the knot positions, and set of control points are constructed. The requirements for B-spline surface are set of control points, set of weights and three sets of knot vectors and are parameterized in the p and q directions.

A Fuzzy B-spline surface $S(p, q)$ is described as a linear combination of basis functions in two topological parameters p and q. Let $R = r_0; \ldots; r_m$ be a nondecreasing sequence of the real numbers. The r_i is called knots and R is the knot vector. The interval r_i and r_{i+1} is called knot span. According to Anile et al. (1995) the Pth-degree (*order* $P+1$) piecewise polynomial function B-Spline basis function, denoted by $\beta_{i,p}(r)$ is given by

$$\beta_{i,1}(r) = \begin{cases} 1 & \text{If } r_i \le r \le r_{i+1}, \\ 0 & \text{otherwise;} \end{cases}$$

$$\beta_{i,P}(r) = \frac{r - r_i}{r_{i+P-1} - r_i}\,\beta_{i,P-1}(r) + \frac{r_{i+P} - r}{r_{i+P} - r_{i+1}}\,\beta_{i+1,P-1}(r)$$

for $P > 1$. (17)

To exercise more shape controllability over the surface, and invariance to perspective transformations, Fuzzy B-spline is introduced. Besides having the control point as in the B-Spline, Fuzzy B-spline also provides a set of weight parameters $w_{i,j}$ that exert more local shape controllability to achieve projective invariance. Following Fuchs et al. (1997) and Russo (1998), Fuzzy B-spline surface that is composed of (OxM) patches is given by

$$S(p,q) = \frac{\sum_{i=0}^{M}\sum_{j=0}^{O} F_O\, C_{ij}\beta_{i,4}(p)\,\beta_{j,4}(q)\,w_{i,j}}{\sum_{m=0}^{M}\sum_{l=0}^{O}\beta_{m,4}(p)\,\beta_{l,4}(q)\,w_{ml}} = \sum_{i=0}^{M}\sum_{j=0}^{O} F_O\, C_{ij}\, S_{ij}(p,q) \quad (18)$$

$\beta_{i,4}(p)$ and $\beta_{j,4}(q)$ are two basis B-spline functions, $\{C_{ij}\}$ are the bidirectional control net and $\{w_{ij}\}$ are the weights. The curve points $S(p,q)$ are affected by $\{w_{ij}\}$ in case of $p \in [r_i, r_{i+P+1}]$ and $q \in [r_j, r_{j+P'+1}]$, where P and P' are the degree of the two B-spline basis functions constituted the B-spline surface. Two sets of knot vectors are *knot* p = $[0,0,0,0,1,2,3,\ldots,O,O,O,O]$, and *knot* q = $[0,0,0,0,1,2,3,\ldots,M,M,M,M]$. Fourth order B-spline basis are used $\beta_{j,4}(.)$ to ensure continuity of the tangents and curvatures on the whole surface topology including at the patches boundaries.

The selected windows of 512×512 pixels and lines (Fig. 1) used to implement Volterra and Fuzzy B-spline models. In order to evaluate the simulation method quantitatively, regression model and root mean square were computed to acquire bathymetry accuracy using TOPSAR data and topographic map of 1998 sheet number 4365 of 1 : 25,000.00 scale.

3 Results and Discussion

Fig. 3 shows regions of interest that were used to simulate bathymetric information by using C-band with VV polarization. The bathymetry information has been extracted from 5 sub-images, each been 512×512 pixels. Fig. 4 shows the signature of underwater topography which can turn up as a result of brightness frontal line parallel to shoreline. Furthermore, it is clear that the front occurred between nearshore and offshore water, which is a clear indications of tidal front events. In fact, the interaction of tidal current with topography can form a tidal front. The TOPSAR backscatter cross-section across front is damped by 0.33 to -7.0 dB. It is known the maximum backscatter values of 0.33 dB is found across the brightness frontal line. Moreover, the variation of radar backscatter cross-section is due to current boundary gradient. According to Vogelzang et al. (1997), ocean current boundaries are often accompanied by the changes in the surface roughness that can be detected by SAR. These surface roughness changes are due to the interaction of surface waves directly with surface current gradients. These interactions can cause an increase in the surface roughness and radar backscatter (Shuchman & Lyzenga 1985 and Wensink & Campbell 1997). Furthermore, these interactions have manifested by bright band in TOPSAR image (Fig. 4). An alternate explanation to bathymetric TOPSAR signature (Fig. 4) that SAR imagine of the bathymetry is only observed in the presence of strong tidal currents. In fact the underwater bottom topography modifies current surface in which the SAR senses these variations. The occurrence of boundary current in the SAR image is contributed to tidal current on order of 0.4 m/s or more. Tidal current flow interacts with the surface waves and thus causing a spatial modulation of Bragg scattering waves. In addition to that, SAR backscattering cross section is proportional to spectra energy density of the Bragg waves, which contributed significantly to imaging mechanism of brightness current boundary (Vogelzang et al. 1992).

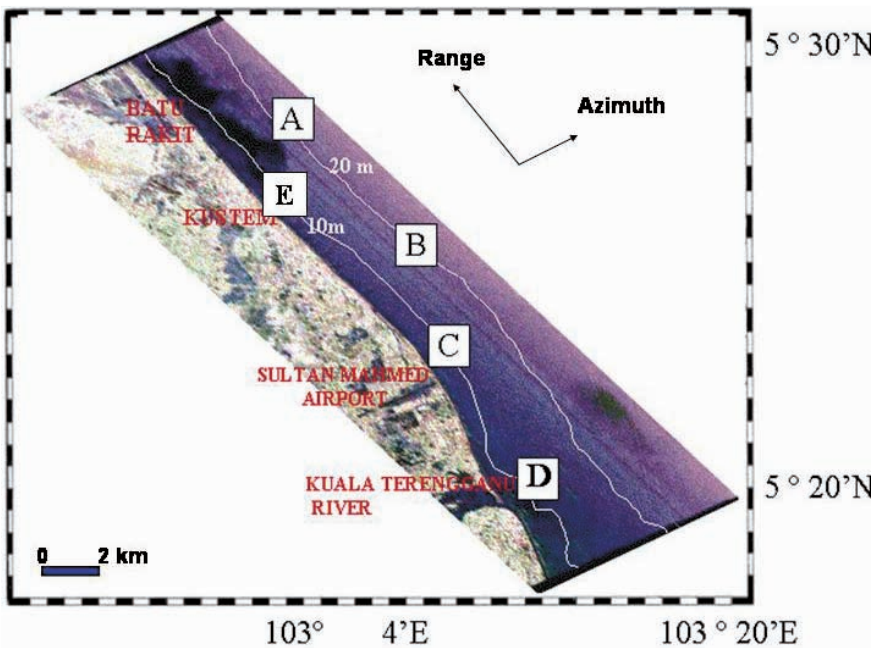

Fig. 3: Selected Window Sizes of A to D with 512 × 512 pixels.

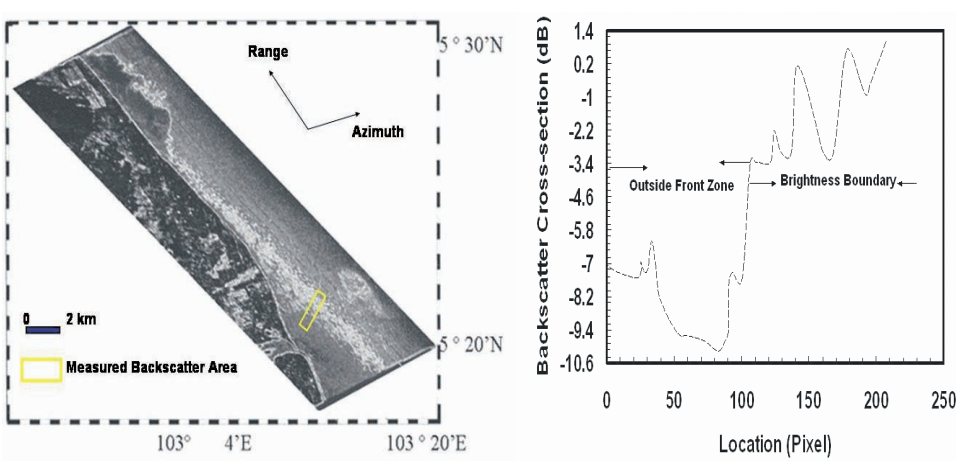

Fig. 4: (a) Bathymetry Signature with C_{vv} Band and (b) Its Backscatter cross-section.

This may provide an explanation of clear bathymetric signatures in TOPSAR C_{VV} band due to strong tidal current flow. Spatial variation of current flow is forced by bathymetric changes. Moreover, continuity equation is used to capture spatial variation of current flow in which is function of water depth. A similar finding was also described by Romeiser & Alpers (1997).

Fig. 5 shows the coastal water current was modelled from C_{VV} by Volterra model. The maximum current velocity was 1.4 m/s which moved from the north direction. In fact December represents the northeast

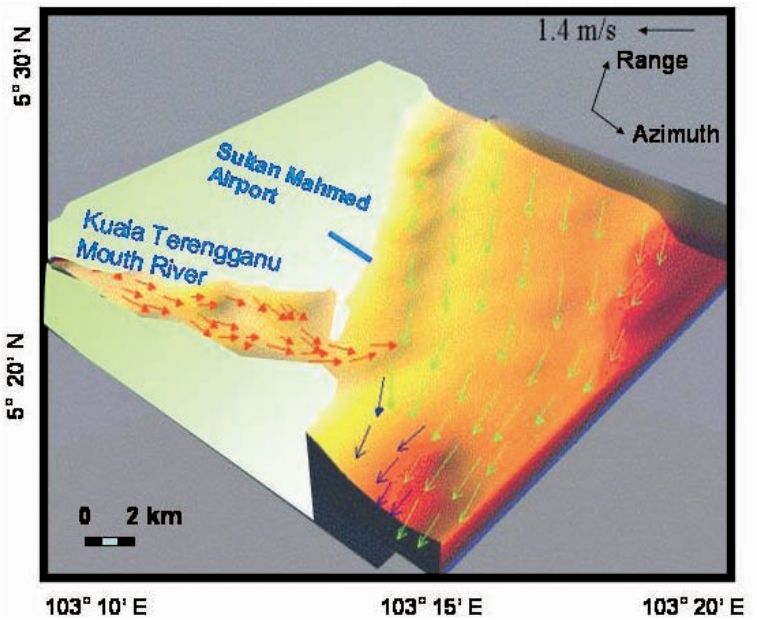

Fig. 5: Current Vectors Simulated from C_{VV} band.

monsoon period as coastal water currents in the South China Sea tend to move from the north direction (MAGED 1994). This proves the recurrence of brightness front was due to strong tidal current flow (Fig. 4). Furthermore, MAGED (1994) quoted that strong tidal current is a dominant feature in the South China Sea with maximum velocity of 1.5 m/s. The range travelling current is due to weak non-linearity caused by the smaller value of R/V which is 32s. The weak non-linearity was assisted by the contribution of linear kernels of range current. This means that the range current will be equal to zero. However, the inversion of linear kernel of Volterra model allowed us to map current movements along the range direction. This result confirmed the study of INGLADA & GARELLO (1999).

Fig. 6 shows the comparison between 3-D bathymetry reconstruction from topography map and C_{VV} band data. It is obvious that the coastal water bathymetry along the Sultan Mahmed Airport has a gentle slopes and moving parallel to the shoreline. Closed to the river mouth, the bathymetry at location shows a sharp slope. The C_{vv} band captured an approximately real bathymetry pattern. This result could be confirmed with regression model in Fig. 7 with R^2 value of 0.62 and accuracy (root mean square) of ± 9 m. This results is strengthened by ANOVA statistical analysis. Statistical analysis shows there is a significant relationship between bathymetry pattern reconstructed from TOPSAR image and topography map, which was shown by the greater value of statistical $F(578)$ than significant $F(0.009)$, with probability value p less than 0.05 (Tab. 1). This confirms the studies of SHUCHMAN et al. (1985) and ROMEISER & ALPERS

Tab. 1: Significant Relationship between TOPSAR and Topography Map.

Statistical Parameters	Values
F	578
Significant F	0.009
P	<0.05
R^2	0.62
RMS	± 9 m

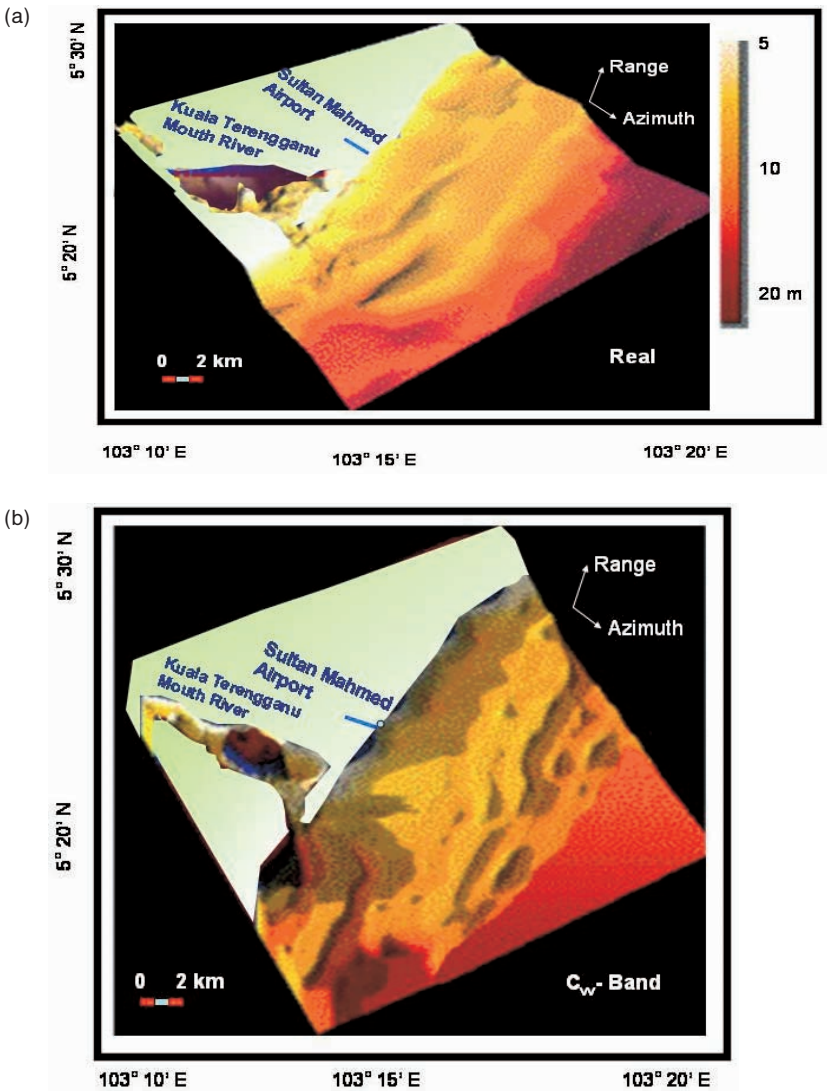

Fig. 6: Three-Dimensional Bathymetry Reconstructions from (a) Real Topography Map and (b) C_{vv} Band.

(1997) which reported C_{vv} band might be used to map coastal water bathymetry. Furthermore, it is interesting to notice that the surface current vectors (Fig. 5) were moved by oblique angle to bathymetry spatial variations (Fig. 6). In fact the bottom topography is not imaged when the bottom feature parallel to current direction (Romeiser & Alpers 1997).

The visualization of 3-D bathymetry is sharp with the TOPSAR C_{vv} band and real data due to the fact that each operations on a fuzzy number becomes a sequence of corresponding operations on the respective μ and μ'-levels, and the multiple occurrences of the same fuzzy parameters evaluated as a result of the function on fuzzy variables (Anile 1997, Anile et al. 1997). It is very

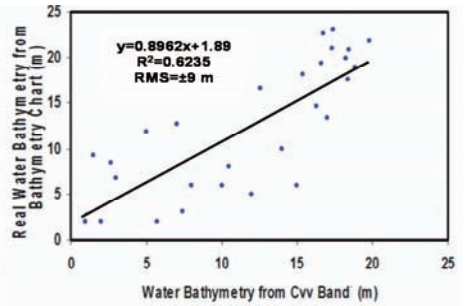

Fig. 7: Regression Model between Real water Bathymetry from Bathymetry Chart and Water Bathymetry from C_{VV} Band.

easy to distinguish between smooth and jagged bathymetry. Typically, in computer graphics, two objective quality definitions for Fuzzy B-splines were used: triangle-based criteria and edge-based criteria. Triangle-based criteria follow the rule of maximization or minimization, respectively, the angles of each triangle. The so-called max-min angle criterion prefers short triangles with obtuse angles. The finding confirms those of KEPPEL (1975) and ANILE (1997). This can be seen in Fig. 6 where the symmetric 3-D structure of the bathymetry of a segment of a connecting depth. Smooth sub-surfaces appear in Fig. 6 where the nearshore bathymetry of 5 m water depth run nearly parallel in 3D-space. A rough subsurface structure appears in steep regions of 20 m water depth. This is due to the Fuzzy B-splines which is considered as a deterministic algorithms. It is described here to optimize a triangulation locally between two different points.

The result obtained in this study disagrees with the previous study by INGLADA & GARELLO (1999 and 2002) who implemented two-dimensional Volterra model to SAR data. 3-D object reconstruction is required to model variation of random points which are function of x, y, and z coordinates. It is incredible to reconstruct 3D using two coordinates i. e. (x, y). In addition, finite element model is required to discretize two-dimensional Volterra and continuity models in study of INGLADA & GARELLO (1999 and 2002) to acquire depth variation in SAR image without uncertainty. Previous studies done by ALPERS & HENNINGS (1984), SHUCHMAN et al. (1985), VOGELZANG et al. (1997), ROMEISER & ALPERS 1997, INGLADA & GARELLO (1999), and HESSELMANS et al. (2000) were able to model spatial variation of sand waves. In this study, Fuzzy B-spline algorithm produced 3-D bathymetry reconstruction without existence of shallow sand waves. In fact Fuzzy B-spline algorithm is able to keep track of uncertainty and provide tool for representing spatially clustered depth points. This advantage of Fuzzy B-spline is not provided in Volterra and continuity models.

4 Conclusion

The utilization of TOPSAR imagery for 3-D bathymetry reconstruction has been implemented by using Volterra and Fuzzy B-spline models. The inversion of Volterra model was used to simulate coastal water current movements. This model was able to acquire maximum surface current value of 1.4 m/s, which within the expected range of current speeds in South China Sea. Strong tidal current speed of 1.4 m/s contributed significantly to the existence of the sharp brightness current boundary in TOPSAR image. In fact the Volterra model was also able to model surface current in two dimensions. Fuzzy algorithm is used to simulate 3-D water depth variation by using one dimensional continuity equation. The fuzzy number values were implemented in B-spline algorithm to reconstruct 3-D bathymetry. Fuzzy B-spline algorithm could visualize the range variations between 5–20 m of water bathymetry. A significant relationship was found between 3-D bathymetry reconstructed using topography map and TOPSAR images. In fact Fuzzy B-spline solved difficulties of spaced grid which is not provided by Volterra model. It can be stated that C_{VV}-band provided bathymetry information is an accurate value of ± 9 m. In conclusion, the integration between Volterra and Fuzzy B-splines models could be an excellent tool for 3-D bathymetry reconstruction.

References

Alpers, W. & Hennings, I., 1984: A theory of the imaging mechanism of underwater bottom topography by real and synthetic aperture radar. – J. Geophys. Res. **89:** 10,529–10,546.

Anile, A.M., Gallo, G. & Perfilieva, I., 1997: Determination of Membership Function for Cluster of Geographical data. – Technical Report No.26/97, 25 p., Institute for Applied Mathematics, National Research Council, Genova.

Anile, A.M., 1997: Report on the activity of the fuzzy soft computing group. – Technical Report of the Dept. of Mathematics, 10 p., University of Catania.

Anile, A.M., Deodato, S. & Privitera, G., 1995: Implementing fuzzy arithmetic. – Fuzzy Sets and Systems, 72.

Fuchs, H., Kedem, Z.M. & Uselton, S.P., 1977: Optimal Surface Reconstruction from Planar Contours. – Communications of the ACM, **20**(10): 693–702.

Hennings, I., Metzner, M. & Calkoen, C.J., 1998: Island Connected sea bed signatures observed by multi-frequency synthetic aperature radar. – International Journal Remote Sensing **19**(10): 1933–1951.

Hesselmans, G.H, Wensink, G.J., Koppen, V., Vernemmen, C. & Cauwenberghe, C.V., 2000: Bathymetry assessment Demonstration of the Belgian Coast-Babel. – The hydrographic Journal **96:** 3–8.

Inglada, J. & Garello, R., 1999: Depth estimation and 3D topography recon-struction from SAR images showing underwater bottom topography signatures. – Proceedings of IGAR SS'99.

Inglada, J. & Garello, R., 2002: On rewriting the imaging mechanism of underwater bottom topography by synthetic aperture radar as a Volterra series expansion. – IEEE Journal of Oceanic Engineering **27**(3): 665–674.

Keppel, E., 1975: Approximation Complex Surfaces by Triangulations of Contour Lines. – IBM Journal of Research Development **19:** 2.

Maged, M., 1994: Coastal Water Circulation of Kuala Terengganu, Malaysia. – MSc. Thesis, Universiti Pertanian Malaysia.

Maged, M., Mohd, H.L. &. Yunus, K., 2002: TOPSAR Model for bathymetry Pattern Detection along coastal waters of Kuala Terengganu, Malaysia. – Journal of Physical Sciences **14**(3): 487–490.

Melba, M., Kumar, S., Richard, M.R., Gibeaut, J.C. & Amy, N., 1999: Fusion of Airborne polarimteric and interferometric SAR for classification of coastal environments. – IEEE Transac-tions on Geoscience and Remote Sensing **37:** 1306–1315.

Romeiser, R. & Alpers, W., 1997: An improved composite surface model for the radar backscattering cross section of the ocean surface, 2, Model response to surface roughness variations and the radar imaging of underwater bottom topography. – J. Geophys. Res. 102,25, 251–25,267.

Russo, F., 1998: Recent advances in fuzzy techniques for image enhancement. – IEEE Transactions on Instrumentation and Measurement **47:** 1428–1434.

Rövid, A., Várkonyi, A.R. & Várlaki, P., 2004: 3D Model estimation from multiple images. – IEEE International Conference on Fuzzy Systems, FUZZY-IEEE'2004, July 25–29, 2004, Budapest, Hungary, pp. 1661–1666.

Schetzen, M., 1980: The Volterra and Wiener theories of nonlinear systems. – John Wiley & Sons, New York.

Shuchman, R.A., Lyzenga, D.R. & Meadows, G.A., 1985: Synthetic aperture radar imaging of ocean-bottom topography via tidal-current interactions: theory and observations. – International Journal Remote Sensing **6:** 1179–1200.

Vogelzang, J., 1997: Mapping submarine sand waves with multiband ima-ging radar. 1, Model development and sensitivity analysis. – J. Geophys. Res. **102:** 1163–1181.

Vogelzang, J., Wensink, G.J., de Loor, G.P., Peters, H.C. & Pouwels, H., 1992: Sea bottom topography with X band SLAR: the relation between radar imagery and bathymetry. – International Journal Remote Sensing **13:** 1943–1958.

Vogelzang, J., Wensink, G.J., Cal-koen, C.J. & van der Kooij, M.W.A., 1997: Mapping submarine sand waves with multiband imaging radar. 2, Experimental results and model comparison. – J. Geophys. Res. **102:** 1183–1192.

Wensink, H. & Campbell, G., 1997: Bathymetric map production using the ERS SAR. – Backscatter **8** (1): 17–22.

Authors' address:

Dr. Maged Marghany
Prof. Dr. Mazlan Hashim
Department of Remote Sensing
Faculty of Geoinformation Science
and Engineering
Universiti Teknologi Malaysia
81310 UTM, Skudai, Johore Bahru,
Malaysia
e-mail: maged@fksg.utm.my
mazlan@fksg.utm.my

Manuskript eingereicht: März 2006
Angenommen: Juli 2006